



# Stem Cell Properties of Gastric Cancer Stem-Like Cells under Stress Conditions Are Regulated via the c-Fos/UCH-L3/ $\beta$ -Catenin Axis

Jae Hyeong Lee<sup>1,4</sup>, Sang-Ah Park<sup>2,4</sup>, Il-Geun Park<sup>2</sup>, Bo Kyung Yoon<sup>3</sup>, Jung-Shin Lee<sup>1,\*</sup>, and Ji Min Lee<sup>2,\*</sup>

<sup>1</sup>Department of Molecular Bioscience, Kangwon National University, Chuncheon 24341, Korea, <sup>2</sup>Graduate School of Medical Science & Engineering, Korea Advanced Institute of Science and Technology, Daejeon 34141, Korea, <sup>3</sup>Department of Biochemistry and Molecular Biology, Yonsei University College of Medicine, Seoul 03722, Korea, <sup>4</sup>These authors contributed equally to this work.

\*Correspondence: jungshinlee@kangwon.ac.kr (JSL); jimin.lee@kaist.ac.kr (JML)

<https://doi.org/10.14348/molcells.2023.0011>

[www.molcells.org](http://www.molcells.org)

Gastric cancer stem-like cells (GCSCs) possess stem cell properties, such as self-renewal and tumorigenicity, which are known to induce high chemoresistance and metastasis. These characteristics of GCSCs are further enhanced by autophagy, worsening the prognosis of patients. Currently, the mechanisms involved in the induction of stemness in GCSCs during autophagy remain unclear. In this study, we compared the cellular responses of GCSCs with those of gastric cancer intestinal cells (GCICs) whose stemness is not induced by autophagy. In response to glucose starvation, the levels of  $\beta$ -catenin and stemness-related genes were upregulated in GCSCs, while the levels of  $\beta$ -catenin declined in GCICs. The pattern of deubiquitinase ubiquitin C-terminal hydrolase-L3 (UCH-L3) expression in GCSCs and GCICs was similar to that of  $\beta$ -catenin expression depending on glucose deprivation. We also observed that inhibition of UCH-L3 activity reduced  $\beta$ -catenin protein levels. The interaction between UCH-L3 and  $\beta$ -catenin proteins was confirmed, and it reduced the ubiquitination of  $\beta$ -catenin. Our results suggest that UCH-L3 induces the stabilization of  $\beta$ -catenin, which is required to promote stemness during autophagy activation. Also, UCH-L3 expression was regulated by c-Fos, and the levels of c-Fos increased in response to autophagy activation. In summary, our findings suggest that the inhibition of

UCH-L3 during nutrient deprivation could suppress stress resistance of GCSCs and increase the survival rates of gastric cancer patients.

**Keywords:** autophagy, cancer stem-like cells, gastric cancer, stress resistance, ubiquitin C-terminal hydrolase-L3

## INTRODUCTION

Gastric cancer has the fifth highest incidence among cancers and the second most common cause of cancer death worldwide. This high mortality in gastric cancer patients is caused by high chemoresistance and recurrence rate, with the probability of cancer recurrence within 5 years after anti-cancer therapy reaching approximately 25% (Fujita, 2009; Joshi and Badgwell, 2021; Rawla and Barsouk, 2019; Torre et al., 2015). It has been proposed that high rates of tumor remodeling and metastasis of gastric cancer are due to gastric cancer stem-like cells (GCSCs), which are a subpopulation of cancer cells sharing stem cell properties (Fu et al., 2018; Zhang et al., 2017).

During tumor remodeling, tumor cells are exposed to various stress signals that activate autophagy, which is an

Received January 12, 2023; revised April 13, 2023; accepted May 24, 2023; published online July 18, 2023

eISSN: 0219-1032

©The Korean Society for Molecular and Cellular Biology.

©This is an open-access article distributed under the terms of the Creative Commons Attribution-NonCommercial-ShareAlike 3.0 Unported License. To view a copy of this license, visit <http://creativecommons.org/licenses/by-nc-sa/3.0/>.

intracellular recycling process. This results in the induction of apoptosis and the inhibition of tumor growth in general. However, recent studies have reported that autophagy can play contrasting roles in tumorigenesis in certain types of cancer (Singh et al., 2018; Xu et al., 2020). They demonstrated that autophagy can promote cancer recurrence and metastasis in tumor tissues characterized by high chemoresistance and metastasis rate (Chen et al., 2022; Xu et al., 2020). This autophagy-mediated tumor induction is due to the reinforcement of stem cell properties by cancer stem cells (CSCs). In the case of gastric cancer, autophagy activates the stemness of GCSCs, the cells responsible for gastric cancer recurrence and metastasis (Chen et al., 2022; Togano et al., 2021). These previous findings suggest that gastric cancer is one of the exceptional cases in the relationship between autophagy and tumor remodeling, and novel approaches are necessary for effective treatments.

On the other hand, it has been reported that autophagy increases the gene expression of  $\beta$ -catenin as well as stem cell properties in tumor tissues (Chen et al., 2022; Dai et al., 2021; Zhu et al., 2021).  $\beta$ -Catenin is a well-studied transcription factor, which induces the expression of the stemness genes (Fan et al., 2016; Lepourcelet et al., 2004; Nusse and Clevers, 2017; Tanabe et al., 2016; Zhang and Wang, 2020). The role of the Wnt/ $\beta$ -catenin pathway in CSC formation is well established (Wang et al., 2017); however, the mechanism of  $\beta$ -catenin signaling enhancement by autophagy is still unclear. Therefore, we hypothesized that deubiquitinases, enzymes that remove ubiquitin from target proteins and increase protein stability, are involved in the induction of autophagy-mediated CSC formation via  $\beta$ -catenin in gastric cancer (Shi et al., 2015; Yang et al., 2019). We further speculated that ubiquitin C-terminal hydrolase-L3 (UCH-L3), the deubiquitinase formerly reported to maintain stem cell properties, could activate  $\beta$ -catenin signaling during autophagy (Lee et al., 2021; Ouyang et al., 2020). However, the crosstalk between UCH-L3 and  $\beta$ -catenin, as well as the mechanism of UCH-L3 regulation, have not been elucidated.

In this study, we investigated the relationship between UCH-L3 activity and GCSC properties during autophagy in gastric cancer cells by comparing the cellular responses of GCSCs with those of gastric cancer intestinal cells (GCICs) that do not exhibit stem cell properties. The cells were cultured in a glucose-deprived medium to mimic tumor micro-environment and promote autophagy (Lin et al., 2020; Shao et al., 2023), which increased protein levels of both UCH-L3 and  $\beta$ -catenin in GCSCs but decreased them in GCICs. The interaction between UCH-L3 and  $\beta$ -catenin proteins was observed, resulting in reduced ubiquitination and increased protein stability of  $\beta$ -catenin. UCH-L3 expression was induced by the transcription factor c-Fos, and the levels of c-Fos increased in response to autophagy activation. Our findings identify a novel potential therapeutic target that could improve the prognosis of gastric cancer patients.

## MATERIALS AND METHODS

### Cell culture and reagent treatment

SNU668, NCI-N87, MKN1, and SNU601 were maintained in

Roswell Park Memorial Institute 1640 medium (RPMI1640, LM011-01; Welgene, Korea) containing 10% fetal bovine serum (FBS, 26140-079; Gibco, USA) and 1% antibiotics (LS203-01; Welgene) at 37°C in a humidified 5% CO<sub>2</sub> incubator. HEK 293T cells were cultured in Dulbecco's modified Eagle's medium (DMEM, LM001-05; Welgene) containing 10% FBS and 1% antibiotics at 37°C in a humidified 5% CO<sub>2</sub> incubator. Trypsin-EDTA 0.25% (LS015-10; Welgene) was used for cell dissociation. The glucose-deprived medium was prepared by mixing glucose-free DMEM (LM001-56; Welgene) with high glucose DMEM (LM001-05; Welgene) in a 9:1 ratio to make 2.5 mM glucose concentration, followed by the addition of 10% FBS and 1% antibiotics. Complete high glucose DMEM with 25 mM glucose (LM001-05; Welgene) containing 10% FBS and 1% antibiotics was used as a control for the glucose starvation condition. TCID (B1467; APEX BIO, USA) and LDN-57444 (S7135; Selleckchem, USA) were dissolved in DMSO and were treated for 24 h in the experiments.

### DNA transfection and RNA interference

The FLAG-UCH-L3 expression plasmid was a kind gift from Prof. Jung Hwa Kim (Inha University, Incheon, Korea) (Lee et al., 2021). The pcDNA3-HA-c-Fos expression and pEGFP-C1- $\beta$ -catenin WT expression plasmids were kind gifts from Prof. SH Baek (Seoul National University, Seoul, Korea). HEK 293T cells were transfected using 1  $\mu$ g/ $\mu$ l polyethyleneimine (PEI, 408727; Sigma, USA), while SNU668 and NCI-N87 cells were transfected using Lipofectamine 3000 (L3000-015; Invitrogen, USA). SNU668 were transfected with siRNA using Lipofectamine 3000. si-FOS (sc-29221) was purchased from Santa Cruz Biotechnology (USA). We purchased siUCH-L3s (SDH-1001, siRNA No. 7347-1, 734-2, 734-3) from Bioneer (Korea) and used pooled siUCH-L3 for our knockdown experiments. Negative control siRNA of Bioneer was used as a transfection control (SN-1003).

### Western blot assay

Cells were collected in cold Dulbecco's phosphate-buffered saline (DPBS, LB001-01; Welgene) and centrifuged at 4°C, 6,000 rpm, for 3 min. The supernatants were removed and pellets were resuspended in lysis buffer EBC200 (50 mM Tris-HCl pH 8.0, 200 mM NaCl, 0.5% NP-40, 100 ng/ml aprotinin, 50 ng/ml leupeptin). Resuspended cells were lysed for 30 min on ice and centrifuged at 4°C, 13,000 rpm, for 10 min. The supernatants were transferred to new tubes for subsequent protein assays. Protein samples were separated using sodium dodecyl sulfate polyacrylamide gel electrophoresis (SDS-PAGE) and transferred to a polyvinylidene fluoride (PVDF) membrane (IPVH00010; Millipore, USA). The transferred membrane was blocked in 1% bovine serum albumin in 0.1% TBS-T for 60 min and then incubated overnight with primary antibodies at 4°C. The antibodies used for these experiments are listed in Table 1.

### Transcriptome analysis

Transcriptomic data of gastric cancer patients were downloaded from the GEO (Gene Expression Omnibus) database (GSE13861 and GSE84437). Microarray data of 497 patients

**Table 1.** List of antibodies used for western blotting

Name	Company	Code
Anti- $\beta$ -catenin antibody	Santa Cruz Biotechnology	#sc7963
Anti-p62 antibody	Cell Signaling Technology	#5114S
Anti- $\beta$ -actin antibody	Sigma	#A5441
Anti-UCH-L3 antibody	Abcam	#ab126703
Anti-UCH-L1 antibody	Santa Cruz Biotechnology	#sc-58595
Anti-Lamin A/C antibody	Cell Signaling Technology	#2032S
Anti- $\alpha$ -tubulin antibody	Abcam	#ab176560
Anti-c-Fos antibody	Cell Signaling Technology	#2250S
Anti-FLAG M2 antibody	Sigma	#3165
Anti-HA antibody	BioLegend	#MMS-101R
Anti-GFP(B20) antibody	Santa Cruz Biotechnology	#sc-9996
Anti-LC3B antibody	Cell Signaling Technology	#2775
Anti-GAPDH antibody	Santa Cruz Biotechnology	#sc-365062

**Table 2.** List of qPCR primers

Primer name	Sequence
Oct4-forward	5'-CGCCCCAGCAGACTTACA-3'
Oct4-reverse	5'-CTCCTCTTTGACCCCTCCCATT-3'
SOX2-forward	5'-AGAGGAGCCCAAGCCAAAGAG-3'
SOX2-reverse	5'-CGAATTCATCCACAGCCGTC-3'
MMP2-forward	5'-ACCCTCAGAGCCACCCCTAA-3'
MMP2-reverse	5'-AGCCAGCAGTGAAAAGCCAG-3'
ZEB2-forward	5'-CCCATTCTGGTTCCTACAGTT C-3'
ZEB2-reverse	5'-GGGAAGAACCCGTCTTGATAT T-3'
hUCH-L3-forward	5'-TGAAGGTCAGACTGAGGCACC-3'
hUCH-L3-reverse	5'-AATTGGAAATGGTTTCCGTCC-3'
hc-FOS-forward	5'-TACTACCACTACCCGCAGAC-3'
hc-FOS-reverse	5'-GAATGAAGTTGGCACTGGAGA-3'
p62-forward	5'-TGCCAGACTACGACTTGTG-3'
p62-reverse	5'-AGTGCCGTGTTTACCTCC-3'
hActB-forward	5'-CACCATTGGCAATGAGCGGTTCC-3'
hActB-reverse	5'-AGGTCTTTGCGGATGTCCACGT-3'
hGAPDH-forward	5'-GACCACTTTGTCAAGCTCATTTCC-3'
hGAPDH-reverse	5'-CTCTCTTCTTGTGCTCTTG-3'
UCH-L3 promoter-forward (containing c-Fos motif)	5'-CAGTGGCCAGAAGAACGTGG-3'
UCH-L3 promoter-reverse (containing c-Fos motif)	5'-GGTAGAGAGCAGTTAGGGAGTC-3'
GAPDH control-forward	5'-CTGCAGTACTGTGGAGGT-3'
GAPDH control-reverse	5'-CAAGGCGGAGTTACCAGAG-3'

were analyzed with R package limma and the expression level is marked as  $\log_2(\text{intensity})$ . Patient annotations are excerpted from the original study (Cheong et al., 2018).

#### Co-immunoprecipitation (co-IP) assay

Cells were lysed in EBC200 lysis buffer containing 100 ng/ml aprotinin and 50 ng/ml leupeptin. Cell extracts were incubated overnight with anti-FLAG M2 antibody (Table 1) at 4°C on a rotator. Lysates were incubated with 30  $\mu$ l of A/G agarose (sc-2003; Santa Cruz Biotechnology) at 4°C for 1.5 h. Next, beads were washed six times with the EBC200 buffer, and proteins were detected by western blotting.

#### RNA isolation and real-time quantitative polymerase chain reaction (qPCR)

Total RNA was extracted using TRIzol Reagent (15596026; Invitrogen), and reverse transcription was performed using a TOPscript™ cDNA Synthesis Kit (EZ005S; Enzynomics, Korea) and MystiCq® microRNA cDNA Synthesis Mix (MIRRT; Sigma) on a T100 thermal cycler (Bio-Rad, USA). Real-time qPCR was performed using TOPreal™ SYBR Green qPCR PreMIX (RT500S; Enzynomics) and QuantStudio 1 (Applied Biosystems, USA) as recommended by the manufacturer's protocols. Gene expression was calculated using the  $\Delta\Delta C_t$  method, and GAPDH and  $\beta$ -actin were used as controls. All reactions were performed in triplicate. The primer sequences used for qPCR are listed in Table 2.

### Cellular protein fractionation

The cells were collected from a culture plate into a cold PBS + EDTA buffer and centrifuged at 4°C, 6,000 rpm for 3 min. Supernatants were removed and cell pellets were resuspended in a Harvest buffer (10 mM HEPES pH 7.9, 50 mM NaCl, 0.5 M sucrose, 0.1 mM EDTA, 0.5% Triton X-100, 1 mM DTT, 10 mM tetrasodium pyrophosphate, 10 mM NaF, 17.5 mM beta-glycerophosphate, 1 mM PMSF, 100 ng/ml aprotinin, 50 ng/ml leupeptin). Resuspended cell pellets were incubated for 5 min on ice and then centrifuged at 4°C 1,000 rpm for 10 min. Supernatants were transferred to new tubes and centrifuged at 4°C, 13,000 rpm, for 10 min. These supernatants contained cytoplasmic proteins. Cell pellets were washed with Buffer A (10 mM HEPES pH 7.9, 10 mM KCl, 0.1 mM EDTA, 0.1 mM EGTA, and freshly added 1 mM DTT, 1 mM PMSF, 100 ng/ml aprotinin, 50 ng/ml leupeptin) and centrifuged at 13,000 rpm for 1 min. Supernatants were discarded and the pellets were resuspended with 4 volumes of Buffer C (10 mM HEPES pH 7.9, 500 mM NaCl, 0.1 mM EDTA, 0.1 mM EGTA, 0.1% NP-40, and freshly added 1 mM DTT, 1 mM PMSF, 100 ng/ml aprotinin, 50 ng/ml leupeptin). The supernatants contained nuclear proteins. Cytoplasmic and nuclear fractions were then examined using western blotting.

### Ubiquitination assay

Cells were transfected with FLAG-UCH-L3 and HA-Ubiquitin and treated with proteasome inhibitor MG132 for 4 h before sample collection. The cells were collected and lysed from lysis buffer (150 mM Tris-HCl pH 8.0, 5% SDS, 10% Glycerol, containing 100 ng/ml aprotinin, 50 ng/ml leupeptin, and 5 mM NEM) for 5 min at room temperature. Lysates were resuspended in the EBC200 buffer containing 100 ng/ml aprotinin, 50 ng/ml leupeptin, and 5 mM N-ethylmaleimide (NEM). Next, lysates were boiled for 15 min and then centrifuged at 13,000 rpm for 10 min. Supernatants were evaluated by co-IP using a HA antibody.

### Chromatin immunoprecipitation (ChIP)

Chromatin immunoprecipitation was performed using HEK 293T cells. Chromatin was sheared on ice by sonication using a Bioruptor apparatus (Diagenode, USA) for six 1-min cycles at a high intensity (200 W) and 20 s off. The size of the sheared chromatin was approximately 200-1,000 bp, as determined by agarose gel electrophoresis. After adding the anti-c-Fos antibody (Table 1), nonspecific binding was blocked by incubation with A/G agarose for 1 h at 4°C. Thereafter, ChIP was performed using a standard protocol. ChIP DNA was analyzed by qPCR using the TOPreal™ SYBR Green qPCR PreMIX (RT500S; Enzynomics) and the 7500 Real-Time PCR System (Applied Biosystems).

### DAPI staining

The cells were fixed with 4% paraformaldehyde for 15 min and then washed two times with PBS. The cells were then stained with 1  $\mu$ g/ml DAPI for 15 min and washed two times with PBS.

### Wound healing

The cells were cultured in a six-well plate until they reached

approximately 90% confluency. After scratching the cell layer with a 200- $\mu$ l pipette tip, the size of the scratches was measured every 24 h.

### Cell viability assay

The cells were seeded at 100,000 cells per well in a six-well plate. The culture medium was changed to 2.5 mM glucose-containing medium, and the number of attached cells was counted every 24 h.

## RESULTS

### GCSC viability does not decrease in response to stress conditions

It has been demonstrated that the stem cell properties and viability of GCSCs were not reduced in a nutrient deprivation environment (Togano et al., 2021). Therefore, we compared the viability of SNU668 (GCSC) and NCI-N87 (GCIC) cell lines cultured in a medium containing a low glucose concentration (2.5 mM). Our results show that SNU668 cells remained viable in response to low glucose conditions, and the cell number was not affected. However, NCI-N87 cells did not tolerate the low glucose environment and the number of cells significantly decreased (Figs. 1A and 1B). These results indicate that GCSCs possess higher resistance to nutrient deficiency than GCICs. Therefore, we speculated that this stress resistance of GCSCs could be related to the increase in stem cell properties (Camuzard et al., 2020; Fu et al., 2018; Zhang et al., 2017).

### Glucose deprivation increases $\beta$ -catenin nuclear accumulation and the expression of stem cell markers

It is well-established that the stem cell characteristics of tumor cells are regulated via several pathways. It has been reported that autophagy enhances the stem cell properties of CSCs in some tumors by upregulating  $\beta$ -catenin (Chen et al., 2022; Takebe et al., 2011; Zhu et al., 2021). Therefore, we evaluated  $\beta$ -catenin levels and stem cell marker expression in gastric cancer cells in response to glucose deprivation. Our results demonstrate that in response to the autophagy activation,  $\beta$ -catenin levels increased in SNU668 cells (GCSCs) and decreased in NCI-N87 cells (GCICs) (Fig. 1C). In addition, the expression of stemness-related genes (OCT4, SOX2, ZEB2, and MMP2) increased in SNU668 cells, corresponding to higher levels of  $\beta$ -catenin (Fig. 1D) (Cole et al., 2008). Additionally, the upregulation of genes related to stemness was verified in MKN1, another type of GCSC, compared to GCICs through glucose deprivation (Supplementary Fig. S1A). These results indicate that the stemness of GCSCs was improved when the levels of  $\beta$ -catenin increased; therefore, we hypothesized that there is a connection between the stem cell properties of GCSCs and  $\beta$ -catenin (Tanabe et al., 2016; Zhang and Wang, 2020). To test this hypothesis, we evaluated  $\beta$ -catenin nuclear translocation in response to glucose deprivation in gastric cancer cells. Our results show that the nuclear levels of  $\beta$ -catenin protein, but not cytoplasmic levels, increased in response to autophagy activation in SNU668 cells (Fig. 1E). These findings suggest that the resistance of GCSCs to stress conditions is due to the expression of the stemness genes induced by increased levels of nuclear  $\beta$ -catenin.

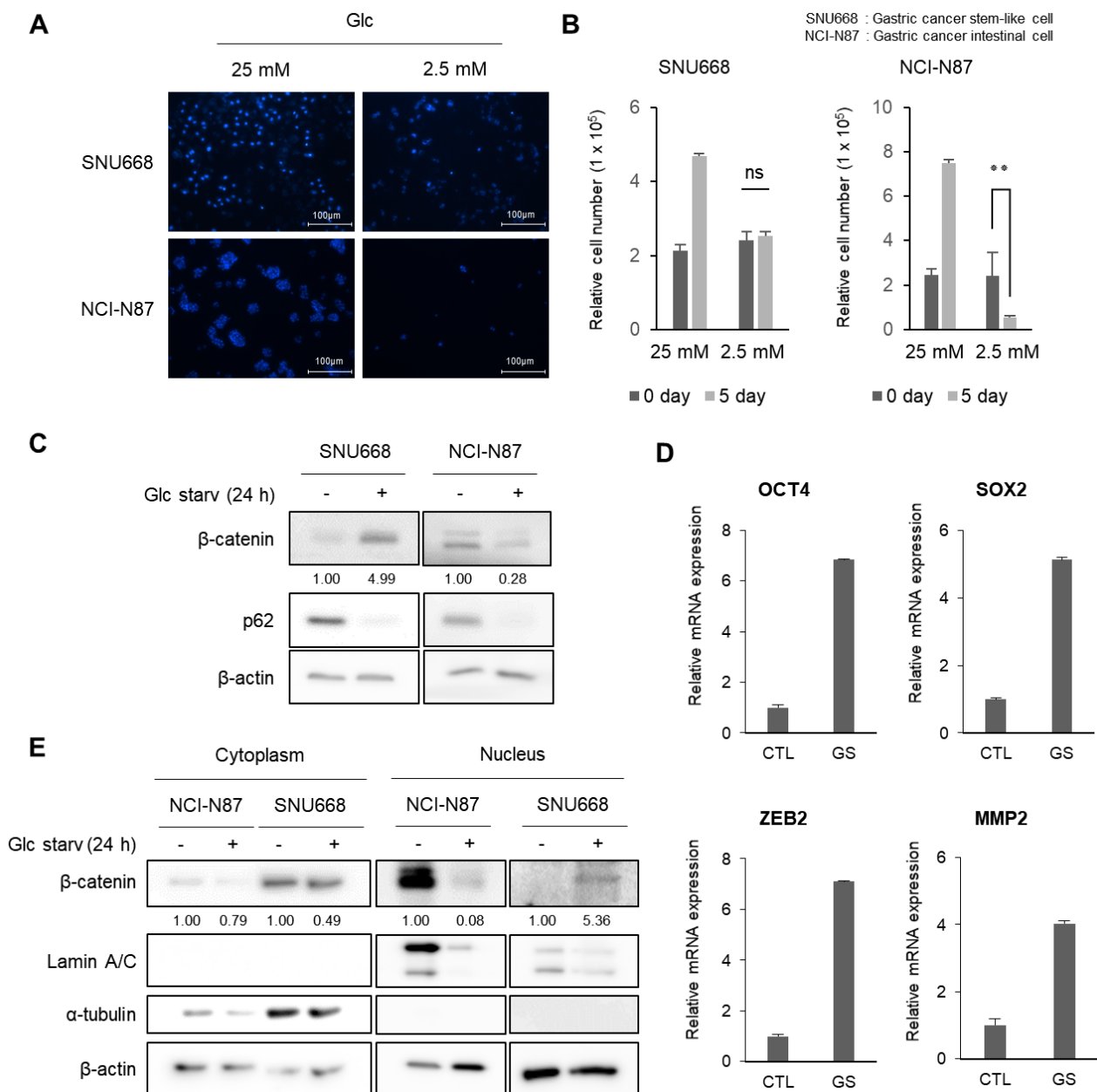


**Fig. 1. Gastric cancer stem-like cells (GCSCs) have a higher survival rate than gastric cancer intestinal cells (GCICs) under stress conditions.** (A) GCSCs and GCICs were cultured in high and low glucose (Glc) (25 mM and 2.5 mM) media for 5 days, and the cell viability was visualized using DAPI staining. (B) Cells (GCSCs and GCICs) were cultured in high and low glucose (25 mM and 2.5 mM) media, and the number of attached cells was counted. Results are expressed as a relative cell number.  $**P < 0.01$ . ns, not significant. (C) Cells (SNU668 and NCI-N87) were cultured in glucose deprivation conditions that induce autophagy activation for 24 h. Western blotting evaluated the protein level of  $\beta$ -catenin; the autophagy marker p62 and  $\beta$ -actin were used as experimental controls. Highly resistant cells (SNU668) show  $\beta$ -catenin induction in response to autophagy. Glc starv, glucose starvation. (D) SNU668 cells were cultured as described in (C), and the expression of stemness-related genes (OCT4, SOX2, ZEB2, and MMP2) was evaluated by qRT-PCR. CTL, control; GS, glucose starvation. (E) Cells (SNU668 and NCI-N87) were cultured as described in (C) and the levels of  $\beta$ -catenin in the cytoplasmic and nuclear extracts were evaluated by western blotting.  $\alpha$ -Tubulin and lamin A/C were used as a cytoplasm and nucleus fraction control, respectively. The relative intensity of the  $\beta$ -catenin signal which is normalized by the  $\beta$ -actin signal is shown below the  $\beta$ -catenin band.

### UCH-L3 promotes stem cell properties by inhibiting $\beta$ -catenin degradation

Our results indicate that the difference between GCSC and

GCIC viability in response to glucose deprivation is due to  $\beta$ -catenin nuclear accumulation. Therefore, there may be endogenous antagonists or blockers in GCSCs that prevent

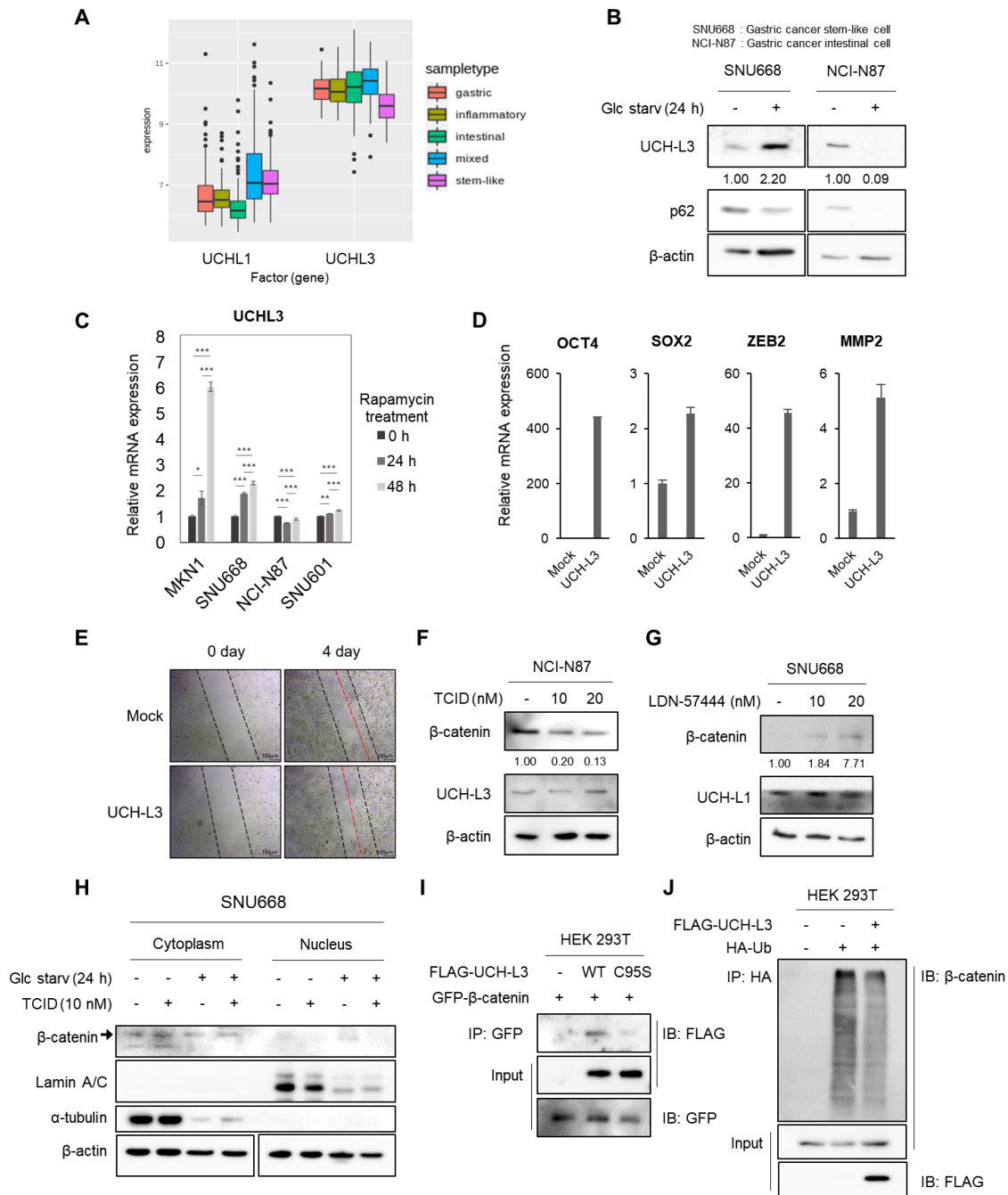


**Fig. 2. Ubiquitin C-terminal hydrolase-L3 (UCH-L3) increases  $\beta$ -catenin nuclear translocation by inhibiting its degradation in response to stress conditions.** (A) Comparison of ubiquitin C-terminal hydrolase-L1 (UCHL1) and UCHL3 mRNA expression levels in tissues of gastric cancer patients. The expression levels of UCHL3 were lower in stem-like tissue than in other tissues. (B) UCH-L3 expression level alteration by glucose starvation (Glc starv) was evaluated by western blotting. This expression pattern was similar to that of  $\beta$ -catenin. (C) The UCHL3 expression levels were measured by RT-qPCR in gastric cancer stem-like cells (MKN1, SNU668) and gastric cancer intestinal cells (NCI-N87, SNU601) treated with 10 nM rapamycin. The data are presented as the mean  $\pm$  SD of three technical replicates. Statistical analysis was performed using a two-tailed *t*-test, and a *P* value of less than 0.05 was considered significant. \**P* < 0.05, \*\**P* < 0.01, \*\*\**P* < 0.005. (D and E) When FLAG-UCH-L3 was overexpressed in SNU668, the expression of stemness-related genes (OCT4, SOX2, ZEB2, and MMP2) and cell migration increased. (F and G) Dose-dependent treatment of the UCH-L3 inhibitor (TCID) reduced the  $\beta$ -catenin protein level in gastric cancer, but the UCH-L1 inhibitor (LDN-57444) did not. (H) Western blotting was used to evaluate  $\beta$ -catenin translocation by a combination treatment of glucose starvation and TCID (10 nM). Autophagy-mediated  $\beta$ -catenin nuclear translocation was blocked by UCH-L3 inactivation. (I) Co-immunoprecipitation (co-IP) was performed to identify the interaction of UCH-L3 and  $\beta$ -catenin. Wild-type (WT) UCH-L3, but not the inactive mutant (C95S), can bind to  $\beta$ -catenin. (J) A ubiquitination assay was used to verify the role of UCH-L3 on  $\beta$ -catenin.

$\beta$ -catenin degradation and allows  $\beta$ -catenin nuclear translocation upon autophagy activation (Yang et al., 2019). Therefore, we investigated the UCH family, known to affect the stemness of cancer cells, in the tissues of gastric cancer patients. Transcriptome profiling dataset GSE13861 and GSE84437 (n = 497) was utilized to investigate the cell type-specific expression of UCH family members, including ubiquitin C-terminal hydrolase-L1 (UCH-L1) and UCH-L3. Our results demonstrate that UCHL3 mRNA expression levels were relatively lower in the stem-like cells of gastric cancer patients than in other cell types. In contrast, UCHL1 mRNA did not exhibit the specific expression pattern of stem-like cells observed in case of UCHL3 (Fig. 2A). Therefore, we hypothesized that the UCH-L3 might be associated with autophagy activation, and first investigated whether autophagy can regulate the UCH-L3 in a cell type-specific manner. In GCSCs (SNU668 and MKN1), UCH-L3 expression levels were low in the control group; however, the expression levels increased in response to glucose deprivation. On the other hand, in GCICs (NCI-N87 and SNU601), UCH-L3 expression

levels decreased in response to autophagy activation (Fig. 2B, Supplementary Fig. S2A). Similarly, while the expression of UCH-L3 significantly increased in GCSCs under autophagy-induced conditions by treating with 10 nM rapamycin, there was no significant change in expression in GCICs (Fig. 2C). Since these changes in UCH-L3 protein levels were similar to  $\beta$ -catenin expression patterns during autophagy activation, we postulated that there may be an association between UCH-L3 and  $\beta$ -catenin.

To test this hypothesis, we investigated whether UCH-L3 could affect the stem cell properties of gastric cancers, similar to  $\beta$ -catenin. Our results show that UCH-L3 overexpression induced the expression of stemness genes (OCT4, SOX2, ZEB2, and MMP2), and increased cell migration (Figs. 2D and 2E). This stemness upregulation by UCH-L3 overexpression was also observed in various gastric cancer cell lines (Supplementary Fig. S1B). Next, we evaluated whether UCH-L3, which enhances the stem cell properties of gastric cancer cells, and UCH-L1, an isotype of UCH-L3 known to promote tumor formation, can also affect  $\beta$ -catenin expression. Our

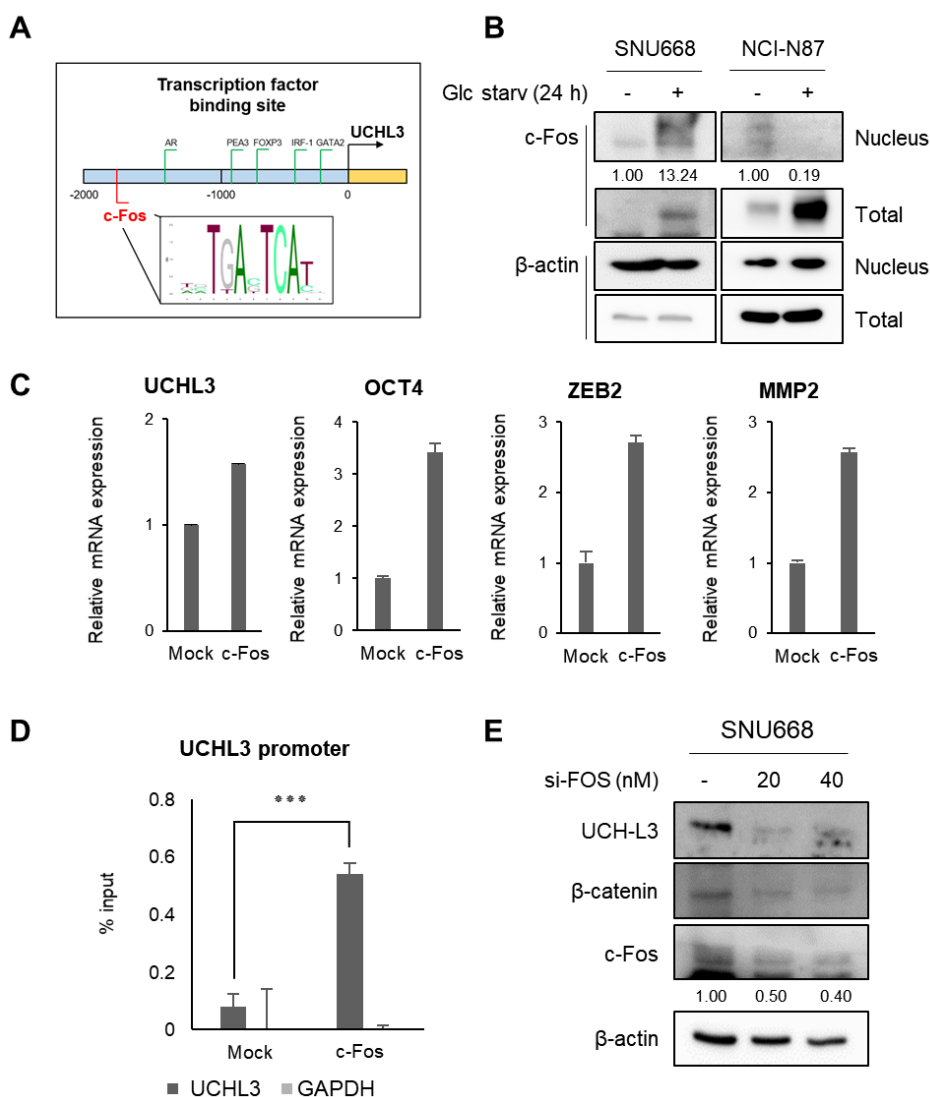


**Fig. 3. c-Fos upregulates ubiquitin C-terminal hydrolase-L3 (UCH-L3) expression, resulting in increased stem cell characteristics of gastric cancer stem-like cells.** (A) The potential binding site of c-Fos in the UCHL3 promoter region. (B) Western blotting was performed to evaluate the c-Fos protein level in response to glucose deprivation. Autophagy-induced c-Fos translocates into the nucleus in SNU668, but not in NCI-N87 cells. Glc starv, glucose starvation. (C) c-Fos overexpression induces transcription of UCHL3 and stemness-related genes (OCT4, ZEB2, and MMP2) in SNU668. (D) ChIP-qPCR was performed to verify the binding of c-Fos to the UCHL3 promoter region.  $***P < 0.001$ . (E) UCH-L3 and  $\beta$ -catenin expression alteration by FOS siRNA was evaluated through western blotting. This result shows that c-Fos-mediated UCH-L3 expression affects  $\beta$ -catenin protein levels.

results indicate that the protein levels of  $\beta$ -catenin decreased in cells treated with TCID, a UCH-L3 inhibitor (Fig. 2F). In addition, the knockdown of endogenous UCH-L3 abrogated the upregulation of  $\beta$ -catenin induced by glucose deprivation (Supplementary Fig. S2B). However,  $\beta$ -catenin levels increased in cells treated with LDN-57444, a UCH-L1 inhibitor (Fig. 2G). To further confirm these findings, the effect of TCID on  $\beta$ -catenin nuclear translocation in SNU668 cells was evaluated. Our results show that, in response to autophagy activation,  $\beta$ -catenin nuclear accumulation was inhibited in the presence of TCID, the UCH-L3 inhibitor (Fig. 2H).

Based on these findings, we hypothesized that UCH-L3 inhibits the degradation of  $\beta$ -catenin and activates the stem cell characteristics of GCSCs by inducing nuclear translocation of  $\beta$ -catenin under stress conditions. Our results demonstrate that there was an interaction between FLAG-UCH-L3 and GFP- $\beta$ -catenin; however, we did not observe this interaction in cells transfected with the inactive mutant of UCH-L3 (UCH-L3 C95S) (Fig. 2I). To examine whether the enzymatic activity of UCH-L3 is directly required for the regulation of  $\beta$ -catenin protein stability, we monitored the half-life of  $\beta$ -catenin by overexpressing UCH-L3 with the treatment of the protein synthesis inhibitor cycloheximide (CHX) (Supplementary Fig. S2C). The overexpression of UCH-L3 extends the half-life of endogenous  $\beta$ -catenin in cells treated with CHX, and treatment of proteasome inhibitor MG132 increased the protein stability of  $\beta$ -catenin in GCSCs (Supplementary Fig. S2D), suggesting that the deubiquitinase activity of UCH-L3 is required for the regulation of  $\beta$ -catenin stability. Furthermore,  $\beta$ -catenin ubiquitination was reduced by the binding of wild-type UCH-L3 (Fig. 2J). Therefore, these findings suggest that the high-stress resistance of GCSCs is due to the increased expression of UCH-L3, which induces  $\beta$ -catenin nuclear translocation by suppressing its degradation; at the same time, GCICs showed relatively low-stress resistance, since UCH-L3 was not expressed.

#### UCH-L3 expression in GCSCs is induced directly by c-Fos

Since the differences in stress responses between GCSCs and GCICs appeared to be due to UCH-L3 expression levels, we stipulated that the regulation of UCH-L3 expression in response to autophagy could suppress cancer recurrence induced by GCSCs. Therefore, to determine the mechanism of UCH-L3 regulation, we investigated transcription factors involved in UCH-L3 expression under glucose deprivation. We analyzed the promoter region of UCHL3 gene and identified a c-Fos binding motif (Fig. 3A). Since c-Fos is a transcription factor expressed during autophagy and known to promote tumorigenesis (Kang et al., 2011; Muhammad et al., 2017; Velazquez et al., 2015), we evaluated the expression of c-Fos under glucose deprivation in gastric cancer cells. Our results show that nuclear c-Fos levels increased in SNU668 cells (GCSCs) in response to glucose starvation, while the levels of nuclear c-Fos in NCI-N87 cells (GCICs) decreased (Fig. 3B). These findings indicated that, unlike in GCICs, c-Fos can translocate into the nucleus in GCSCs in response to autophagy, and consequently affect downstream gene expression.

The c-Fos overexpression not only increased the transcription of UCHL3, but also of stemness-related genes such as

OCT4, ZEB2, and MMP2 (Fig. 3C). Using ChIP-qPCR, we confirmed that this increased UCH-L3 gene expression is caused by direct binding of c-Fos to the UCH-L3 promoter (Fig. 3D). Next, to further verify the mechanism, we suppressed c-Fos expression using siRNA. Our results show that the downregulation of c-Fos levels decreased the level of  $\beta$ -catenin, as well as that of UCH-L3 (Fig. 3E), suggesting that UCH-L3 directly induced by c-Fos affects  $\beta$ -catenin protein levels. These results indicate that the nuclear translocation of c-Fos promotes stem cell properties by enhancing the expression of UCH-L3 in GCSCs (SNU668) under stress conditions. However, in GCICs (NCI-N87), the absence of c-Fos translocation did not affect UCH-L3 levels, leading to poor environmental resistance compared to GCSCs.

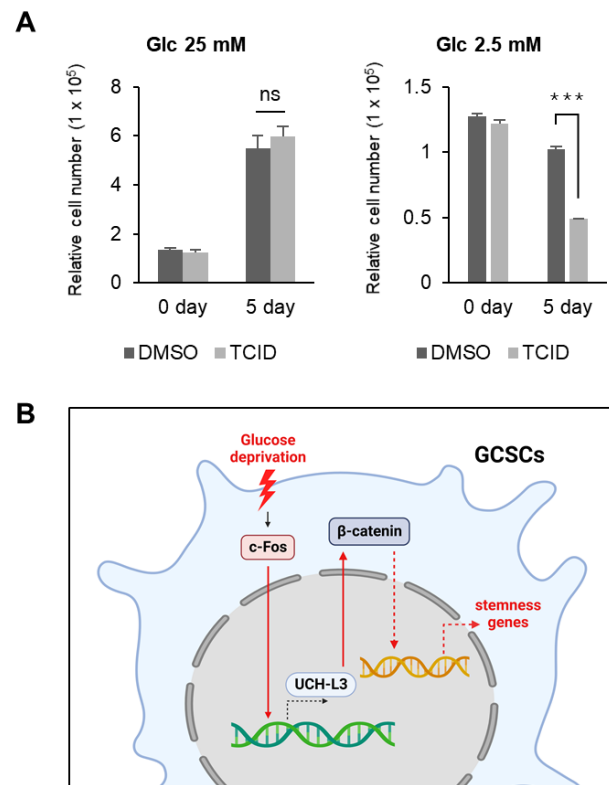


**Fig 4. In response to stress, c-Fos regulates UCH-L3 expression, resulting in  $\beta$ -catenin stabilization and the subsequent induction of gastric cancer stem-like cell (GCSC) stem cell properties.** (A) SNU668 was cultured in high and low glucose (25 mM and 2.5 mM) media and TCID (10 nM) combined media for 5 days and the survival cell number was compared. Decline of survival cells by UCH-L3 inactivation was observed under glucose deprivation conditions only. \*\*\* $P < 0.001$ . ns, not significant. (B) Schematic diagram of the proposed mechanism. In response to autophagy activation (glucose deprivation), c-Fos translocates into the nucleus and promotes UCH-L3 expression. High levels of UCH-L3 inhibit  $\beta$ -catenin degradation, and stabilized  $\beta$ -catenin enhances the stem cell properties of GCSCs.



### UCH-L3 activity is necessary for maintaining the stem cell properties of GCSCs in response to stress

Our findings indicate that the high-stress resistance of GCSCs is due to increased expression of UCH-L3, leading to higher  $\beta$ -catenin protein stability. Therefore, we investigated whether the inhibition of UCH-L3 activity can reduce the resistance of GCSCs under stress conditions. Our results demonstrate that the viability of SNU668 cells (GCSCs) significantly reduced in response to UCH-L3 inhibitor treatment. However, this decrease in cell viability was observed only under the low glucose (2.5 mM) condition and not under the normal glucose (25 mM) condition (Fig. 4A). Collectively, we suggest that UCH-L3 is actively involved in regulating the stem cell properties of gastric cancer cells under stress conditions only, such as nutrient deprivation, and not under normal conditions. Therefore, the high resistance of GCSCs to the stress environment is maintained through c-Fos-mediated upregulation of UCH-L3 expression. However, when UCH-L3 activity is inhibited under stress conditions, the viability of GCSCs becomes similar to that of GCICs (Fig. 4B).

## DISCUSSION

Tumor tissues are highly dynamic and formed by a combination of CSCs and non-CSCs. The high chemoresistance of CSCs is the major cause of cancer metastasis (Fu et al., 2018; Li et al., 2014; Yu et al., 2012). In gastric cancer, the stem cell characteristics of GCSCs are induced by autophagy, leading to high recurrence rates and patient mortality after anti-cancer therapy (Nazio et al., 2019; Togano et al., 2021; Zhang et al., 2017).

Previous studies have shown that autophagy is required to maintain CSC properties, and an increase in  $\beta$ -catenin levels promotes the formation of CSCs (Chen et al., 2022; Dai et al., 2021; Fan et al., 2016; Tanabe et al., 2016; Zhu et al., 2021). These findings were also observed in gastric cancer. Here, we report that GCSCs increased nuclear protein levels of  $\beta$ -catenin in response to autophagy activation and were highly resistant to stress conditions (Lepourcelet et al., 2004; Tanabe et al., 2016; Togano et al., 2021). In contrast,  $\beta$ -catenin levels were reduced by autophagy activation in GCICs, the cells with relatively low-stress resistance. This difference in  $\beta$ -catenin levels was due to c-Fos, a transcription factor activated by autophagy. In GCSCs, c-Fos translocated into the nucleus and induced UCH-L3 expression under stress conditions, resulting in the inhibition of  $\beta$ -catenin degradation. In GCICs, the c-Fos nuclear translocation did not occur in response to stress conditions, leading to low UCH-L3 expression levels and increased degradation of  $\beta$ -catenin. Therefore, we confirmed that the difference in resistance to the stress environment in these two gastric cancer cell types is caused by the expression levels of UCH-L3, which in turn stabilized  $\beta$ -catenin. Furthermore, the viability of GCSCs decreased under stress conditions in response to the inhibition of UCH-L3 activity (Fig. 4B).

The regulation of cell viability by UCH-L3 was only observed under stress conditions, while the inhibition of UCH-L3 under non-stress conditions did not affect cell proliferation. Similarly, UCH-L1, a member of the UCH family known to

promote tumor growth and the deubiquitinating enzyme highly expressed in GCSCs (Gu et al., 2015; Lee et al., 2021; Lu et al., 2021; Yang et al., 2015), negatively affected the expression of  $\beta$ -catenin. Therefore, we speculated that the stem cell properties of gastric cancer cells under normal conditions were maintained through pathways other than  $\beta$ -catenin (Gu et al., 2015; Takebe et al., 2011). However, it is possible that  $\beta$ -catenin signaling activated by UCH-L3 is required to maintain the stem cell properties of GCSCs during autophagy-activating conditions, such as nutrient deprivation.

In summary, we suppose that the suppression of UCH-L3 could effectively limit gastric cancer recurrence after surgery by preventing GCSC induction. Furthermore, to effectively inhibit UCH-L3, the pathways that induce c-Fos translocation and regulate UCH-L3 transcription, as well as epigenetic changes that could affect the expression of c-Fos target genes, should be investigated. In conclusion, we demonstrated that the expression of UCH-L3 in GCSCs under stress conditions is induced by c-Fos, resulting in nuclear accumulation of  $\beta$ -catenin, and conferring high resistance to external stimuli by expressing stemness genes. Therefore, we propose that the inhibition of UCH-L3 activity after anti-cancer therapy could suppress tumor remodeling and metastasis, providing a new strategy to improve the prognosis of gastric cancer patients.

*Note: Supplementary information is available on the Molecules and Cells website (www.molcells.org).*

## ACKNOWLEDGMENTS

This work was supported by the Basic Science Research Program NRF-2021R1C1C1008780 to J.M.L. from the National Research Foundation (NRF) grant funded by the Korean government.

## AUTHOR CONTRIBUTIONS

J.H.L. was involved in the execution of the study and was primarily responsible for writing the manuscript. J.H.L., S.-A.P., and I.-G.P. conducted the research and wrote the manuscript. B.K.Y. performed transcriptome analysis. J.-S.L. and J.M.L. supervised the study.

## CONFLICT OF INTEREST

The authors have no potential conflicts of interest to disclose.

## ORCID

Jae Hyeong Lee	<a href="https://orcid.org/0000-0003-3225-6556">https://orcid.org/0000-0003-3225-6556</a>
Sang-Ah Park	<a href="https://orcid.org/0009-0001-9179-0647">https://orcid.org/0009-0001-9179-0647</a>
Il-Geun Park	<a href="https://orcid.org/0009-0009-8315-9044">https://orcid.org/0009-0009-8315-9044</a>
Bo Kyung Yoon	<a href="https://orcid.org/0000-0003-3436-4665">https://orcid.org/0000-0003-3436-4665</a>
Jung-Shin Lee	<a href="https://orcid.org/0000-0002-9126-5463">https://orcid.org/0000-0002-9126-5463</a>
Ji Min Lee	<a href="https://orcid.org/0000-0003-2978-2440">https://orcid.org/0000-0003-2978-2440</a>

## REFERENCES

- Camuzard, O., Santucci-Darmanin, S., Carle, G.F., and Pierrefitte-Carle, V. (2020). Autophagy in the crosstalk between tumor and microenvironment. *Cancer Lett.* 490, 143-153.
- Chen, Y., Zhao, H., Liang, W., Jiang, E., Zhou, X., Shao, Z., Liu, K., and Shang, Z. (2022). Autophagy regulates the cancer stem cell phenotype of head

- and neck squamous cell carcinoma through the noncanonical FOXO3/SOX2 axis. *Oncogene* 41, 634-646.
- Cheong, J.H., Yang, H.K., Kim, H., Kim, W.H., Kim, Y.W., Kook, M.C., Park, Y.K., Kim, H.H., Lee, H.S., Lee, K.H., et al. (2018). Predictive test for chemotherapy response in resectable gastric cancer: a multi-cohort, retrospective analysis. *Lancet Oncol.* 19, 629-638.
- Cole, M.F., Johnstone, S.E., Newman, J.J., Kagey, M.H., and Young, R.A. (2008). Tcf3 is an integral component of the core regulatory circuitry of embryonic stem cells. *Genes Dev.* 22, 746-755.
- Dai, X.M., Zhang, Y.H., Lin, X.H., Huang, X.X., Zhang, Y., Xue, C.R., Chen, W.N., Ye, J.X., Lin, X.J., and Lin, X. (2021). SIK2 represses AKT/GSK3 $\beta$ /beta-catenin signaling and suppresses gastric cancer by inhibiting autophagic degradation of protein phosphatases. *Mol. Oncol.* 15, 228-245.
- Fan, D., Ren, B., Yang, X., Liu, J., and Zhang, Z. (2016). Upregulation of miR-501-5p activates the wnt/beta-catenin signaling pathway and enhances stem cell-like phenotype in gastric cancer. *J. Exp. Clin. Cancer Res.* 35, 177.
- Fu, Y., Du, P., Zhao, J., Hu, C., Qin, Y., and Huang, G. (2018). Gastric cancer stem cells: mechanisms and therapeutic approaches. *Yonsei Med. J.* 59, 1150-1158.
- Fujita, T. (2009). Gastric cancer. *Lancet* 374, 1593-1594; author reply 1594-1595.
- Gu, Y.Y., Yang, M., Zhao, M., Luo, Q., Yang, L., Peng, H., Wang, J., Huang, S.K., Zheng, Z.X., Yuan, X.H., et al. (2015). The de-ubiquitinase UCHL1 promotes gastric cancer metastasis via the Akt and Erk1/2 pathways. *Tumour Biol.* 36, 8379-8387.
- Joshi, S.S. and Badgwell, B.D. (2021). Current treatment and recent progress in gastric cancer. *CA Cancer J. Clin.* 71, 264-279.
- Kang, W., Tong, J.H., Chan, A.W., Lee, T.L., Lung, R.W., Leung, P.P., So, K.K., Wu, K., Fan, D., Yu, J., et al. (2011). Yes-associated protein 1 exhibits oncogenic property in gastric cancer and its nuclear accumulation associates with poor prognosis. *Clin. Cancer Res.* 17, 2130-2139.
- Lee, J.E., Lim, Y.H., and Kim, J.H. (2021). UCH-L1 and UCH-L3 regulate the cancer stem cell-like properties through PI3 K/Akt signaling pathway in prostate cancer cells. *Anim. Cells Syst. (Seoul)* 25, 312-322.
- Lepourcelet, M., Chen, Y.N., France, D.S., Wang, H., Crews, P., Petersen, F., Bruseo, C., Wood, A.W., and Shivdasani, R.A. (2004). Small-molecule antagonists of the oncogenic Tcf/beta-catenin protein complex. *Cancer Cell* 5, 91-102.
- Li, M., Zhang, B., Zhang, Z., Liu, X., Qi, X., Zhao, J., Jiang, Y., Zhai, H., Ji, Y., and Luo, D. (2014). Stem cell-like circulating tumor cells indicate poor prognosis in gastric cancer. *Biomed Res. Int.* 2014, 981261.
- Lin, X., Xiao, Z., Chen, T., Liang, S.H., and Guo, H. (2020). Glucose metabolism on tumor plasticity, diagnosis, and treatment. *Front. Oncol.* 10, 317.
- Lu, G., Li, J., Ding, L., Wang, C., Tang, L., Liu, X., Xu, J., Zhou, Q., Sun, J., Wang, W., et al. (2021). The deubiquitinating enzyme UCHL1 induces resistance to doxorubicin in HER2+ breast cancer by promoting free fatty acid synthesis. *Front. Oncol.* 11, 629640.
- Muhammad, N., Bhattacharya, S., Steele, R., Phillips, N., and Ray, R.B. (2017). Involvement of c-Fos in the promotion of cancer stem-like cell properties in head and neck squamous cell carcinoma. *Clin. Cancer Res.* 23, 3120-3128.
- Nazio, F., Bordi, M., Cianfanelli, V., Locatelli, F., and Cecconi, F. (2019). Autophagy and cancer stem cells: molecular mechanisms and therapeutic applications. *Cell Death Differ.* 26, 690-702.
- Nusse, R. and Clevers, H. (2017). Wnt/beta-catenin signaling, disease, and emerging therapeutic modalities. *Cell* 169, 985-999.
- Ouyang, L., Yan, B., Liu, Y., Mao, C., Wang, M., Liu, N., Wang, Z., Liu, S., Shi, Y., Chen, L., et al. (2020). The deubiquitylase UCHL3 maintains cancer stem-like properties by stabilizing the aryl hydrocarbon receptor. *Signal Transduct. Target. Ther.* 5, 78.
- Rawla, P. and Barsouk, A. (2019). Epidemiology of gastric cancer: global trends, risk factors and prevention. *Prz. Gastroenterol.* 14, 26-38.
- Shao, Y., Ren, W., Dai, H., Yang, F., Li, X., Zhang, S., Liu, J., Yao, X., Zhao, Q., Sun, X., et al. (2023). SKP2 contributes to AKT activation by ubiquitination degradation of PHLPP1, impedes autophagy, and facilitates the survival of thyroid carcinoma. *Mol. Cells* 46, 360-373.
- Shi, J., Liu, Y., Xu, X., Zhang, W., Yu, T., Jia, J., and Liu, C. (2015). Deubiquitinase USP47/UBP64E regulates beta-catenin ubiquitination and degradation and plays a positive role in Wnt signaling. *Mol. Cell. Biol.* 35, 3301-3311.
- Singh, S.S., Vats, S., Chia, A.Y., Tan, T.Z., Deng, S., Ong, M.S., Arfuso, F., Yap, C.T., Goh, B.C., Sethi, G., et al. (2018). Dual role of autophagy in hallmarks of cancer. *Oncogene* 37, 1142-1158.
- Takebe, N., Harris, P.J., Warren, R.Q., and Ivy, S.P. (2011). Targeting cancer stem cells by inhibiting Wnt, Notch, and Hedgehog pathways. *Nat. Rev. Clin. Oncol.* 8, 97-106.
- Tanabe, S., Aoyagi, K., Yokozaki, H., and Sasaki, H. (2016). Regulation of CTNBB1 signaling in gastric cancer and stem cells. *World J. Gastrointest. Oncol.* 8, 592-598.
- Togano, S., Yashiro, M., Masuda, G., Sugimoto, A., Miki, Y., Yamamoto, Y., Sera, T., Kushiyama, S., Nishimura, S., Kuroda, K., et al. (2021). Gastric cancer stem cells survive in stress environments via their autophagy system. *Sci. Rep.* 11, 20664.
- Torre, L.A., Bray, F., Siegel, R.L., Ferlay, J., Lortet-Tieulent, J., and Jemal, A. (2015). Global cancer statistics, 2012. *CA Cancer J. Clin.* 65, 87-108.
- Velazquez, F.N., Caputto, B.L., and Boussin, F.D. (2015). c-Fos importance for brain development. *Aging (Albany N.Y.)* 7, 1028-1029.
- Wang, H., Duan, X.L., Qi, X.L., Meng, L., Xu, Y.S., Wu, T., and Dai, P.G. (2017). Concurrent hypermethylation of SFRP2 and DKK2 activates the Wnt/beta-catenin pathway and is associated with poor prognosis in patients with gastric cancer. *Mol. Cells* 40, 45-53.
- Xu, J.L., Yuan, L., Tang, Y.C., Xu, Z.Y., Xu, H.D., Cheng, X.D., and Qin, J.J. (2020). The role of autophagy in gastric cancer chemoresistance: friend or foe? *Front. Cell Dev. Biol.* 8, 621428.
- Yang, F., Xu, J., Li, H., Tan, M., Xiong, X., and Sun, Y. (2019). FBXW2 suppresses migration and invasion of lung cancer cells via promoting beta-catenin ubiquitylation and degradation. *Nat. Commun.* 10, 1382.
- Yang, H., Zhang, C., Fang, S., Ou, R., Li, W., and Xu, Y. (2015). UCH-L1 acts as a novel prognostic biomarker in gastric cardiac adenocarcinoma. *Int. J. Clin. Exp. Pathol.* 8, 13957-13967.
- Yu, Z., Pestell, T.G., Lisanti, M.P., and Pestell, R.G. (2012). Cancer stem cells. *Int. J. Biochem. Cell Biol.* 44, 2144-2151.
- Zhang, L., Guo, X., Zhang, D., Fan, Y., Qin, L., Dong, S., and Zhang, L. (2017). Upregulated miR-132 in Lgr5(+) gastric cancer stem cell-like cells contributes to cisplatin-resistance via SIRT1/CREB/ABCG2 signaling pathway. *Mol. Carcinog.* 56, 2022-2034.
- Zhang, Y. and Wang, X. (2020). Targeting the Wnt/beta-catenin signaling pathway in cancer. *J. Hematol. Oncol.* 13, 165.
- Zhu, Y., Huang, S., Chen, S., Chen, J., Wang, Z., Wang, Y., and Zheng, H. (2021). SOX2 promotes chemoresistance, cancer stem cells properties, and epithelial-mesenchymal transition by beta-catenin and Beclin1/autophagy signaling in colorectal cancer. *Cell Death Dis.* 12, 449.